ICAS-84-3.7.2

FATIGUE CRACK INITIATION AND MICROCRACK PROPAGATION IN NOTCHED AND UNNOTCHED ALUMINIUM 2024-T3 SPECIMENS

J. Foth[1], R. Marissen[2], H. Nowack[2] and G. Lütjering[3]

1) IABG, D-8012 Ottobrunn, formerly DFVLR, D-5000 Köln 90, FRG
2) DFVLR, D-5000 Köln 90, FRG
3) Technische Universität Hamburg-Harburg, D-2100 Hamburg-Harburg, FRG

Abstract

The fatigue behaviour of notched and unnotched Al 2024-T3 specimens was investigated, where the same strain history was applied at the notch root of the notched specimens and at the surface of the unnotched specimens (according to the equivalence concept by Crews and Hardrath). The number of cycles to crack initiation and the growth rates of the microcracks were determined. The microcracks usually started at the hard intermetallic Fe- and Si-containing inclusions which are present in the commercial 2024-T3 alloy. For an analytical description of the growth behaviour of the small cracks equivalent stress intensity factors were introduced which are based on the J-integral by Rice and which could be used to perform crack propagation calculations together with an Elber type equation.

In the case of notched specimens the stress gradient is of special importance.

Under variable amplitude loading histories considerable load sequence effects occured, both in the crack initiation and in the macrocrack propagation stage. These could be predicted, if a new damage parameter concept by Hanschmann was used for the pre-crack stage and a calculation method for the short crack stage which especially accounted for the opening behaviour of the cracks

Introduction

Due to economic reasons materials for aerospace applications are selected such that the weight of the structures can be kept as low as possible without any loss in the reliability which is required. Because high strength aluminium alloys show both, good mechanical strength properties and a low specific weight, and because the manufacturing costs of structural parts are low as compared to other high strength materials, aluminium alloys are extensively utilized since a long time.[1] Although some structural parts may go into service, which already exhibit crack-like defects, usually no visible cracks are present at the beginning of the life time. After some time in service microcracks may be initiated, preferably at notches or other stress raisers, and start to grow.[2] They are hardly detectable until they become macrocracks. For the consideration of the macrocracks, fracture mechanics based analyses are usually applied. For these types of analyses it has usually to be assumed that the material is homogeneous and behaves isotropically. Provided that the mechanical environment of the cracks remains predominantly elastic during the fatigue life of structural parts, the stress intensity factor represents a quite useful (one-parametric) tool to predict the macrocrack behaviour for different types of test pieces and crack geometries and for different loading conditions on the basis of the conventional da/dN vs. ΔK curves of the material.

It has to be pointed out, however, that under fatigue loading in the limited life range a considerable part of the total life is spent in the small crack stage. If the behaviour of small cracks is compared to that of macrocracks, there exist several important differences which do not allow for a simple straight forward application of the macrocrack principles to the short crack stage.[3-8] In the literature it is reported that the propagation rates of short cracks are often higher than expected on the basis of long crack data. Sometimes so-called non-propagating cracks can be initiated especially in the case of sharp notches.[8] The threshold value for fatigue crack propagation is different for short cracks as compared to long cracks.[4-7] Microstructural parameters become of special importance for smaller cracks. If the size of the short cracks reaches the order of magnitude of a grain size or of inclusions the prediction capability of simple fracture mechanics based analyses decreases. If notches are present which cause gradients of the stresses and of the strains, these gradients have a strong effect, as well.

Under variable amplitude loading a non-linear damage accumulation is observed. The damage and the crack growth per cycle do not depend only on the mean stress and on the amplitude of the instantaneous load cycle, but also on the previous loading history. Such so-called sequence effects were observed for the engineering crack initiation stage (which covers the pre-crack stage and the small crack stage)[9,10] as well as for the macrocrack stage.[11,12] However, it is still widely unknown, how these sequence effects become active in the pre-crack stage and in the short crack stage themselves.

In the present study it is tried to make some further contributions to a better understanding of the still widely unknown damage processes in the pre-crack and in the microcrack stages. It is further tried to derive special fracture mechanics mechanics based concepts for the characterization of the microcrack behaviour.

In order to work out the influence of notches and to further evaluate the ranges in the applicability of modern notch analysis concepts the life behaviour of both notched specimens and of unnotched specimens has been investigated, whereby the same strain history was applied at the notch root of the notched specimens and along the gage length of an unnotched specimen according to the equivalence concept which was originally proposed by Crews and Hardrath.[13]

Experimental Program

In the present study the following types of fatigue tests were performed on double edge notched (K_t = 1.22 and K_t = 3.3) specimens and an unnotched (K_t = 1.0) specimen which were taken from flat Al 2024-T3 sheets with a thickness of 4.7 mm (compare Fig.1).

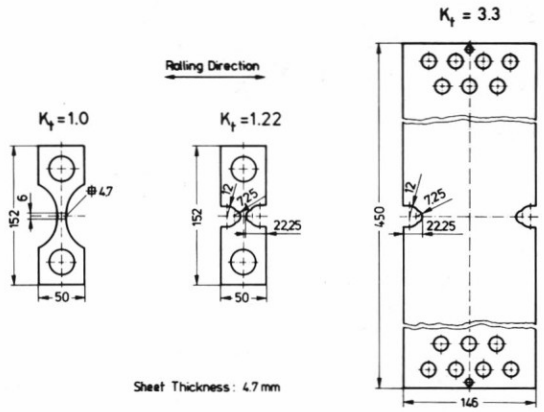

FIGURE 1. Al 2024-T3 sheet specimens as they were used in the present study.

The technical Al 2024-T3 alloy contains Fe and Si impurities from the manufacturing process. These impurities form coarse intermetallic inclusions with the alloying elements.

For the experimental programs on the notched and on the unnotched specimens two different types of constant amplitude strain histories, $\epsilon = 0.7 \pm 0.3$ % and $\epsilon = 0.85 \pm 0.15$ % , respectively, were applied at the notch root of the notched specimens and along the gage length of the unnotched specimens. Besides that tests with simple variable amplitude histories were performed which represented combinations of the two constant amplitude histories.

For the observation of the crack initiation and of the crack propagation behaviour in the course of the tests light-microscopes were applied (compare also[3,14]). After the tests further microstructural investigation including scanning electron microscope analyses were performed.

Results and discussion

Phenomenological aspects of the crack initiation process

For most of the commercial aluminium alloys the coarse intermetallic inclusions are of predominant importance for the initiation of fatigue cracks, as it was already mentioned before.[15-18] These hard intermetallic inclusions cause inhomogeneous plastic deformations within the surrounding matrix material because of different mechanical properties of the inclusions and of the matrix material. Usually the inclusions fracture after some time and microcracks start to grow from these inclusions.

In Fig. 2 the crack initiation and the short crack propagation is shown as it was observed in tests with the K_t = 3.3 specimen. On the basis of the light-microscopical investigations four different individual stages can be distinguished:

-stage I: Initiation of very small cracks which are irregularly distributed along the specimen surface, and which cannot be easily identified by the use of light-microscopes. The number of microcracks is much larger as compared to the number of those cracks which later form the macrocrack. Stage I is defined to be ended as soon as some of the intermetallic inclusions have been broken and microcracks of a length of 5 - 10 µm are present.

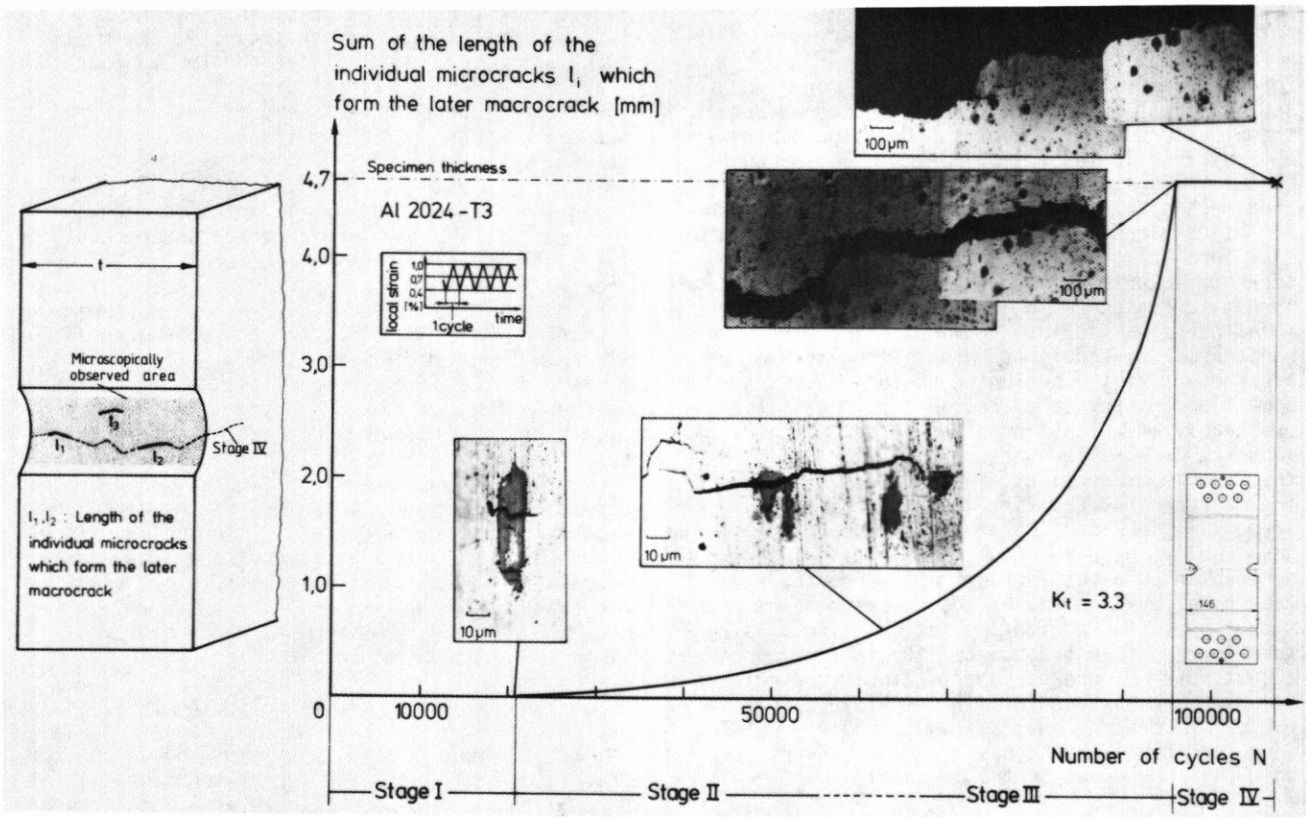

FIGURE 2. Initiation and propagation behaviour of small cracks which later form the macrocrack.

- stage II: Growth of the microcracks. The microcracks now become clearly visible by means of light-microscopes. In Fig. 2 the sum of the lengths of only those individual microcracks which later form the macrocrack is plotted on the ordinate. Stage II ends as soon as some of the small cracks form into a line which is identical to the path of the macrocrack which forms lateron.

- stage III: The small cracks now coalesce. At the end of stage III the whole surface is is cut through by one predominant crack.

- stage IV: The predominant crack becomes clearly visible at the side surface of the specimen now and represents a conventionally propagating macrocrack.

If the duration of the individual stages is compared for the applied strain history, stage I ends after about 30 % of the total life time. The small crack stages (stage II and stage III) cover about 65 % of the total life. Only about 15 % of the total life is spent in the macrocrack stage. If the loading conditions are changed, these proportions can alter to some extent. The test results in Fig. 2 clearly show the significance of the microcrack stage. Along with the engineering treatment of technical problems quite often different subdivisions of the total life into individual parts are performed, depending on the applied construction philosophy ("Damage tolerance design", or "no macrocracks permitted" (the latter is a very convenient principle for the machine designing branches or for the automotive industry)) and also depending on the NDT methods which can be made available to detect cracks. There usually exist considerable sources of inaccuracies - except for stage IV, the macrocrack stage - where special inspections of the damage progression become possible.

Regarding the microstructural processes in the four stages some informative results have already been published elsewhere.[3,11,14,19]

Influence of notches on the crack initiation and on the microcrack propagation stage

As already indicated modern notch analysis concepts assume that notches and unnotched specimens behave in an equivalent manner, if the same local strain histories are applied at the fatigue critical areas. In order to examine this concept further, the same strain histories were generated at all three types of the specimens by the aid of highly accurate strain measurement procedures. Fig. 3 shows the $\Sigma l_{i,net}$ vs. N (for definition see left part of Fig.2) curves for the K_t = 1.0, K_t = 1.22 and K_t = 3.3 specimens in the constant strain amplitude tests with $\epsilon = 0.7 \pm 0.3$ %. It can be seen that the three specimens show approximately the same life until crack initiation (stage I). However, the propagation behaviour of the cracks in the stages II - IV becomes significantly different: at the unnotched specimens the cracks propagate much faster than at the notched specimens. The total number of small cracks which are initiated at the unnotched specimens is larger, as well, because the total gage length and the whole cross-section of the unnotched specimens are loaded with the same strain. The crack growth was lower for the K_t = 1.22 specimens, and the lowest crack growth was observed for the K_t = 3.3 specimens. At the K_t = 1.0 and K_t = 1.22 specimens no significant stable crack propagation

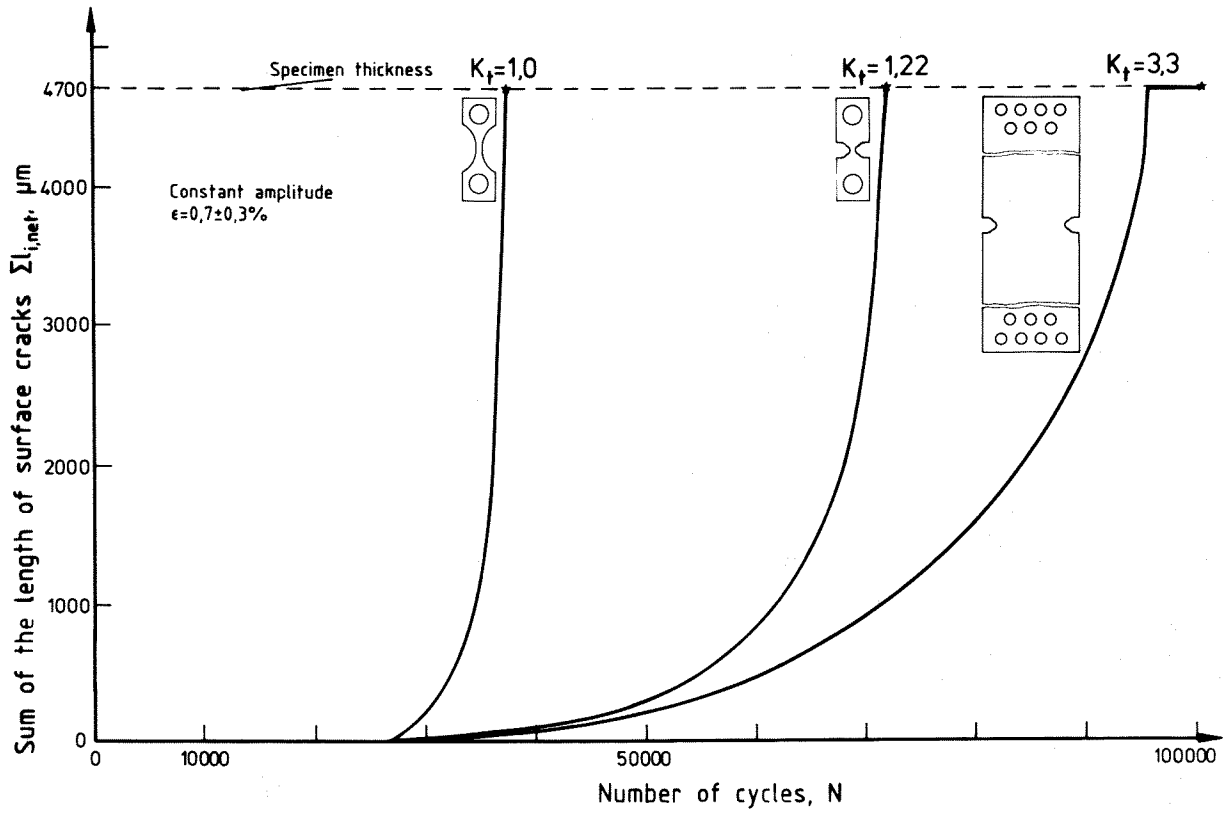

FIGURE 3. Crack initiation and microcrack propagation for the three different types of Al 2024-T3 specimens which were considered in the present study.

could be observed at the side surfaces of the specimens.

The fact that the life in the crack stages increases as the notch factor increases is mainly due to the presence of the stress gradient: The stresses decrease as the cracks propagate into the bulk material. The unnotched specimens do not exhibit a stress gradient.

Fig. 4 gives the results of a three-dimensional finite element calculation of the stresses for the K_t = 1.22 specimen.[20] One eighth of the actual specimen is shown in the figure, and the origin point of the coordinate system represents the middle of the notch. It can be seen that the highest stresses occur in the middle of the notch, and at this location most of the microcracks actually start to grow.

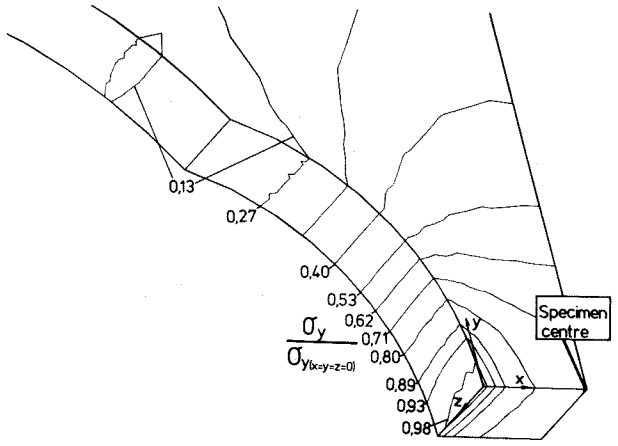

FIGURE 4. Elastic stress distribution at the K_t = 1.22 specimen from a finite element calculation[20] (one eighth-representation of the specimen).

If the results of the second test series are considered, where a (local) strain history of $\epsilon = 0.85 \pm 0.15$ % (instead of $\epsilon = 0.7 \pm 0.3$ %) was applied, it is to be seen that the approximate equivalence of the fatigue behaviour in stage I which was observed for the $\epsilon = 0.7 \pm 0.3$ % history now considerably decreases.[14,19] The K_t = 1.22 and the K_t = 3.3 specimens show no cracks below a mean value of the life data of $2 \cdot 10^6$. The unnotched specimens, however, show failures in most cases. A similar trend (a decreasing equivalence in the fatigue behaviour with decreasing load level) was also observed in [12,13,21,22]. An explanation of this behaviour may be the presence of a size effect, because the volume of the material at and close to the surface which is stressed at the high level is larger for the unnotched specimens than for the notched specimens. Besides that specimens, where gradients of the local stresses and strains are present, are usually able to rebuild local stress peaks due to a redistribution of the stresses towards areas where stresses are still at a lower level.

Description of the propagation behaviour of small cracks

Constant amplitude loading

The previous sections have shown that the small crack stage is of special importance for the fatigue life behaviour of specimens and components. That is the main reason why analytical fracture mechanics based analyses for this stage are required.

For such analyses the following boundary conditions have to be considered especially: The cracks initiate at inclusions and propagate as semielliptical or semicircular surface cracks. That means that the whole problem is three-dimensional. The actual stress/strain distributions are furtheron influenced by the shape of the crack and of the test piece. The stress gradients which are present in the vicinity of stress raisers are of importance, as well. Besides that the closure behaviour of the short cracks has to be accounted for, and in a very close connection with the crack closure behaviour stands the influence of the instantaneous R-value. In order to show the significance of the last mentioned point more clearly (long crack) da/dN- ΔK curves of the Al 2024.T3 alloy are given for different R-values in Fig. 5. It can be seen that all data are on one line, if they are plotted vs. the effective stress intensity range in the tests after Elber's concept[23], where the crack closure behaviour is especially taken into account.

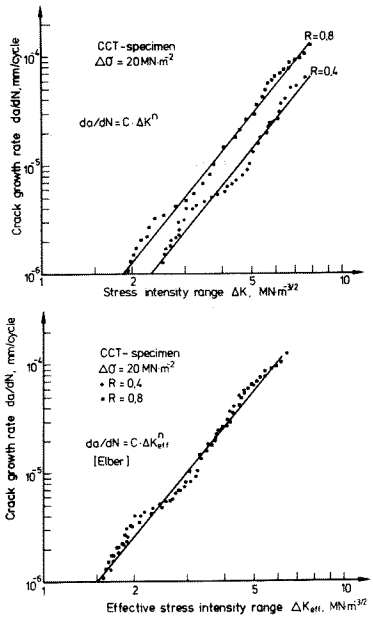

FIGURE 5. Crack growth rates of Al 2024-T3 for different R-ratios, plotted vs. ΔK and vs. ΔK_{eff} after Elber's equation, respectively.

In order to consider the effects of the instantaneous shape of the crack and of the stress gradient as being present in the vicinity of the notches, the following superposition concept on the basis of similarity considerations as it is shown in Fig. 6 is suggested here. K_{NEC}, the stress intensity factor for a semielliptical surface crack within a notch field is determined by taking the stress intensity

factor of a semielliptical surface crack in an unnotched specimen K_{EC} (which can be calculated on the basis of Newman's approximate calculations in [24]) and by multiplying K_{EC} by K_{NCC}/K_{CC}. The exact solution for the stress intensity factor K_{CC} can be taken from the literature. The stress gradient has to be considered by a polynomial equation which may be derived from finite element calculations of the stress distribution of the notched specimens.[20] Using a numerical integration of solutions which are also reported in the literature (compare [25]), K_{NCC} can be determined.

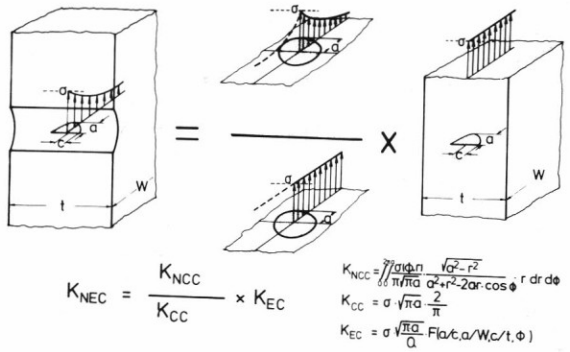

FIGURE 6. Calculation concept for the stress intensity factor for semielliptical surface cracks within a notch field.

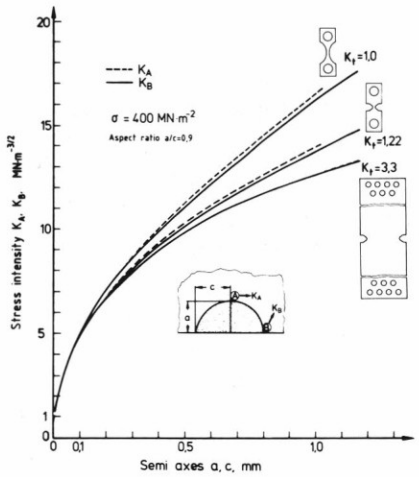

FIGURE 7. Stress intensity factors at A (deepest point) and B (surface) for semielliptical surface cracks.

If the described procedure is applied to the specimens in the present study the behaviour in Fig. 7 becomes visible. (In the figure the stress intensity factors at the crack tip, K_A, and the stress intensity factor at the specimen/notch surface, K_B, are plotted vs. the semi axes of the crack ellipse.) The curves clearly indicate that the instantaneous amount and the increase in the stress intensity factor as a function of the instantaneous semi axes of the crack ellipse are the largest for the unnotched specimens and lower for the notched specimens. This coincides with the observed trends in the crack propagation behaviour in Fig. 3.

From a mechanics' point of view the instantaneous shape of the small cracks has a significant influence on the stress intensity factor. If the crack is assumed to be semicircular (a = c), it comes out that K_A is smaller than K_B - and if it is assumed that the instantaneous crack shape is like a flat ellipse, K_A is larger than K_B. The small cracks preferrably grow into the direction with a higher stress intensity. That means, that after some times always a certain equilibrium condition is reached. For this equilibrium condition the theoretical a/c-ratio is 0.89. Fig. 8 shows the described tendency, and also experimental data which coincide with the analytical trends.

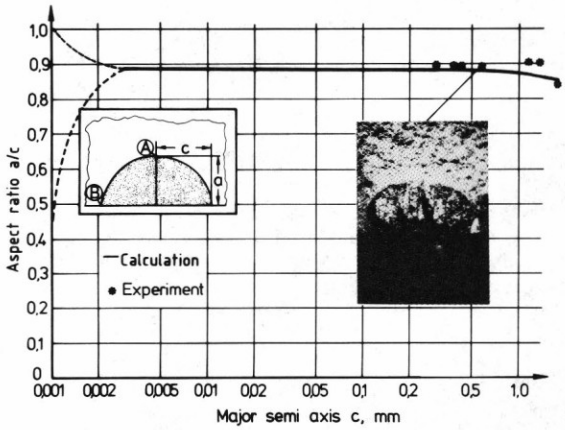

FIGURE 8. Shape of the semielliptical surface cracks as a function of the crack length.

On the basis of the analytical anlyses which are described so far, calculations of the growth rates of small cracks become possible using long crack da/dN vs. ΔK curves as basic input data as long as larger plastic deformations do not occur in the surroundings of the small cracks. In the present study, however, larger plastic deformations occured during the first increase in the strain up to ϵ_o = 1.0 % (σ_o = 390 MN·m^{-2}) during the first half of the first cycle. During the following half cycles the surface strain varied between ϵ_o = 1 % and ϵ_u = 0.4 % (σ_u = - 8 MN·m^{-2}) and remained predominantly elastic. For these half cycles a ΔK-based concept may become applicable. However, the value of the maximum stress intensity after the first increase in the strain has to be determined firstly. In order to extend the range where linear elastic fracture mechanics principles can be applied, the J-integral by Rice[26] is often successfully used. The J-integral for an elliptical crack or for a semielliptical surface crack within a stress field with a stress gradient can be determined using a solution proposed by Shih and Hutchinson[27]. In this approach the material stress-strain behaviour is considered by a Ramberg-Osgood type equation:

$$\epsilon = \frac{\sigma}{E} + A \cdot \sigma^b \qquad (1)$$

For the aluminium alloy 2024-T3 the material parameters E, A and b are: E = 72500 MN·m^{-2}, A = $1.37 \cdot 10^{-31}$ and b = 11, respectively.

The J-integral for cross-section stresses at the test pieces being smaller than the yield strength of the material is:

$$J = \frac{\pi \cdot a \cdot \sigma^2}{E} + \frac{\pi \cdot a}{2 \cdot E} \cdot \left(\frac{b-1}{b+1}\right) \cdot \left(\frac{\sigma}{\sigma_F}\right)^2 \cdot \sigma^2 + a \cdot g_1 \cdot A \cdot \sigma^{b+1} \qquad (2)$$

or

$$J = \frac{\pi \cdot a \cdot \sigma^2}{E} + \frac{\pi \cdot a}{2 \cdot E} \cdot \left(\frac{b-1}{b+1}\right) \cdot \sigma^2 + a \cdot g_1(0,b) \cdot A \cdot \sigma^{b+1} \qquad (3)$$

if the cross-section stresses are higher than the yield strength of the material. In these equations g_1 can be determined by:

$$g_1 = 3.85 \cdot b \cdot \sqrt{1 - \frac{1}{b}} + \frac{\pi}{b} \qquad (4)$$

Using the equations (1),(3) and (4) the amount of the J_{max}-value after the first decrease in the load can now be determined. This calculated J_{max}-value (and any other J-value which may follow in the further course of the loading history) is now formally transformed into an equivalent stress intensity factor K^+ using the convenient equation:

$$K^+ = \sqrt{E \cdot J} \qquad (5)$$

For all other load cycles after the first half cycle up to ϵ_o = 1 % (where the strain varies between ϵ_o = 1 % and ϵ_u = 0.4 %) the hysteresis behaviour of the material and the Bauschinger effect have to be considered, if further K^+-values (K^+_{min}, K^+_{max}, K^+_{min} etc.) are determined by a half cycle-by-half cycle application of the J-integral calculation procedure.

This procedure is not in general accordance with the basic definition of the J-integral by Rice. However, it is quite reasonable to assume, that the change of the stress state at the crack tip due to the consecutive half cycles is described in an adequate manner by the proposed procedure. In the present case the cyclic loading after the first half cycle caused predominantly elastic deformations only. That means, that LEFM-calculations may be sufficient, as well.

Based on the considerations so far, a sequence of K^+_{max} and K^+_{min}-values for a given loading history can be determined. These K^+-values offer a physically more reasonable basis for the evaluation of the crack propagation behaviour in the case of elastic-plastic loading conditions as compared to the conventional approach which considers the stresses and the stress ratio $R = \sigma_u/\sigma_o$. This is further substantiated by the fact that the K^+_{min}/K^+_{max}-ratio is quite similar to the $R_\epsilon = \epsilon_u/\epsilon_o$-ratio, as it is present in the tests in this study (compare Fig. 9).

Furthermore it seemed reasonable to assume that the influence of the elastic-plastic deformations during the first half cycle (which are accounted for by the K^+_{max}-value) remains further effective for the following fatigue loading over the entire range of the crack length, and that the Elber type equation can also further be used together with the instantaneous K^+_{min}/K^+_{max}-ratio - or the strain ratio $R_\epsilon = \epsilon_u/\epsilon_o$, respectively.

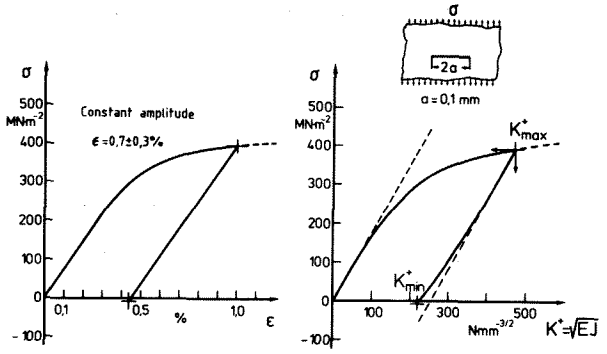

FIGURE 9. Cross-section stress vs. strain and vs. the range of the equivalent stress intensity factor K^+, which has been determined on the basis of an elastic-plastic J-integral consideration.

It has to be pointed out again, that the proposed concept is an approximative procedure.

Fig. 10 shows the growth behaviour of the microcracks at the surface of unnotched specimens, and Fig. 11 shows the microcrack growth behaviour at the surface of the most severely notched specimen (K_t = 3.3). The squared symbols in the figures represent the test results. The dashed lines are averaging curves through the experimental results. Also shown in the figures are crack growth calculations using the Elber type equation, once using the conventional stress ratio being present in the tests, and once by applying the procedure as it was explained above (R_ϵ-concept). It can be seen that crack growth calculations based on the conventional stress ratio remain unsatisfactorily for the entire range of the crack lengths (dash-dotted line). The solid line shows the calculation results using the strain ratio $R_\epsilon = \epsilon_u/\epsilon_o$. This line describes the test results quite well in their trend except for very short crack lengths, where the crack growth rates are somewhat underestimated. Here a "short crack effect" is becoming visible, as it is reported in the literature for crack lengths which approach microstructural sizes like the grain size or inclusion sizes[4-8]. At large crack lengths the crack growth predictions deviate from the actual test results, as well. This may be contributed to the fact that there occurs a delay in the crack growth at the specimen surface, because the large cracks form due to the coalescence of several smaller semielliptical surface cracks, the depth of which is much smaller than the depth of the coalesced stabilized crack later on. The situation becomes more clearly if Fig. 12 is considered, where the crack growth behaviour of two different types of semielliptical surface cracks has been compared, which exhibited both the same surface crack length of l = 2c = 2 mm, but different depths of 0.9 (equilibrium condition) and of 0.45 mm, respectively. It can be seen that the crack with the ratio of the semi axes of a/c = 0.9 shows the higher crack growth rates at the specimen surface rather than the crack with the flat semielliptical shape. In the stage II and III the crack propagation takes place predominantly by the coalescence of smaller individual cracks, each of which exhibits a much smaller size of the semi axis a (crack propagation into the interior of the specimen) than the semi axis of the coalesced crack which has already

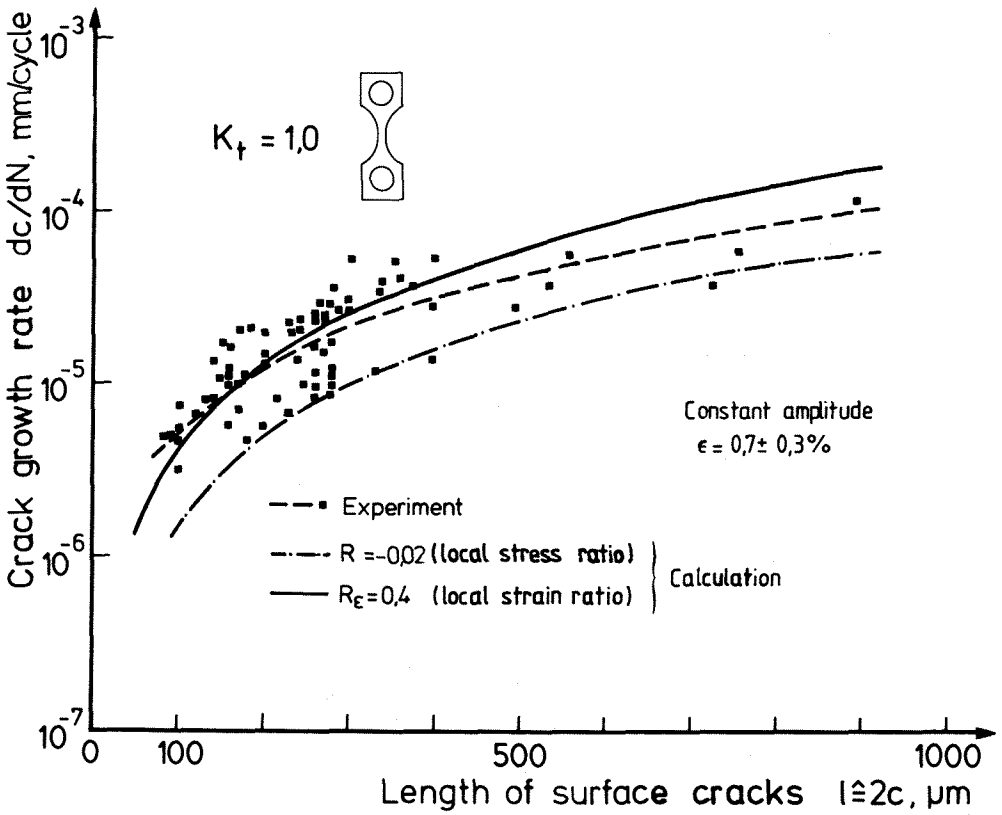

FIGURE 10. Small crack behaviour at the surface of the unnotched Al 2024-T3 specimens in strain controlled tests. (c = major semi axis of the crack ellipse).

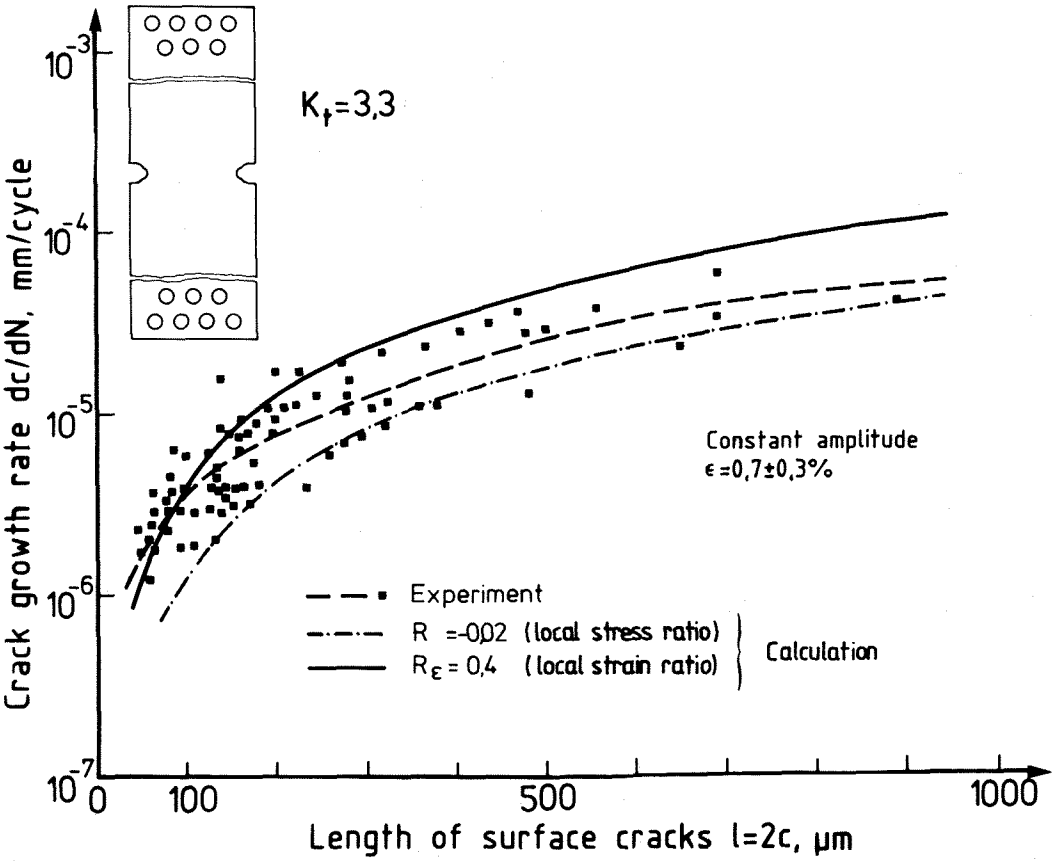

FIGURE 11. Growth behaviour of the small surface cracks for the K_t = 3.3 specimens.

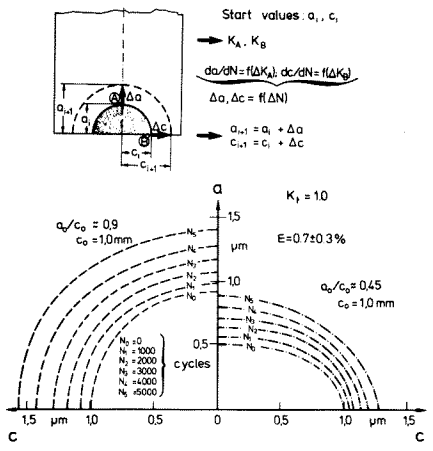

FIGURE 12. Comparison of the propagation behaviour of surface cracks with two different initial shapes of the surface cracks.

reached the equilibrium condition. This may explain the experimentally observed slower crack growth rates of the "larger" microcracks (end of stage II/ stage III-cracks) as compared to the calculation with the strain ratio until they approach the equilibrium condition (stable crack shape).

If the results of the previous section are summarized it can be stated that for surface cracks with a range in their crack lengths between l = 2c = 50 µm (this is about 2 - 4 times the grain size) up to l = 500 µm the crack growth predictions using the equivalent stress intensity factor concept and using long crack da/dN vs. ΔK data worked satisfactorily.

Crack growth behaviour under variable loading conditions

For the evaluation of the crack growth behaviour under loading histories where the amplitudes and mean stresses vary, two procedures are of special interest (compare Fig. 13) which are described on the basis of a "biharmonic" loading history, as it was applied in the present study:

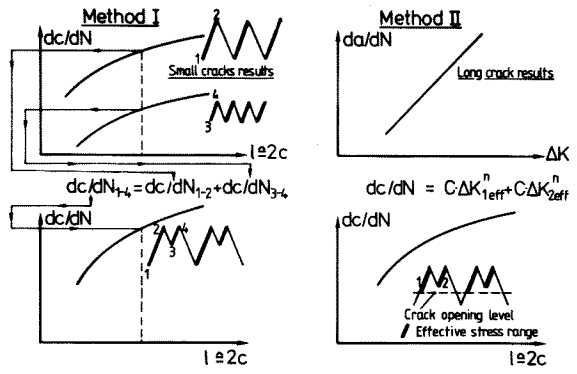

FIGURE 13. Two methods for the evaluation of the crack growth behaviour under biharmonic loading history.

Method I:

The crack growth increments per biharmonic cycle are calculated by a linear summation of the crack growth increments, dc/dN_{1-2} and dc/dN_{3-4}, whereby dc/dN_{1-2} and dc/dN_{3-4} are taken on the basis of the experimental behaviour as it was observed in constant amplitude (small crack) tests with the mean stress and with the amplitude of the larger load variations only, and with the mean stress and with the amplitude of the smaller cycles only, respectively. Such a very simple form of damage calculation is often used in the engineering design.

Method II:

The crack growth predictions are performed using da/dN vs.ΔK data as a basic input (these data are determined with long crack experiments). In order to especially account for the crack opening behaviour the effective ΔK-range is used which is calculated on the basis of the stress ratio for predominantly elastic situations or on the basis of the K^+_{min}/K^+_{max}-ratio or the strain ratio R_ϵ as proposed in the present study for situations where the crack environment becomes elastic-plastic. The crack growth increments per cycle are further influenced by the load sequence . Under "biharmonic loading the crack opening load level is in particular controlled by the large stress variations in the cycle. This is the reason why during the smaller cycles within the large cycles the crack is always fully open. This method was already proposed for macrocrack growth predictions at variable amplitude fatigue loading.[28]

In Fig. 14 the predictions after both methods are compared with the actual test results for the K_t = 1.22 specimens. It can be seen that the experimental crack growth data tend to be larger than the predictions after method I over the entire range in the crack lengths. A linear summation of constant amplitude data does not sufficiently account for the changes in the amount of the damage due to the sequence effects under variable amplitude loading conditions. Similar sequence effects are extensively known also from long crack investigations.[11,12,28,29] In the present case the damage is significantly increased due to the small cycles.

The predictions after method II (based on long crack data) show the same tendency as already observed under constant amplitude loading conditions (compare Figs. 11, 12), namely, that the predictions are lower at very short crack lengths and that they become higher as the crack lengths become larger. Altogether the predictions after method II slightly tend into the conservative direction. The reasons for the deviations in the predictions after method II at very short and at relatively large crack lengths from the actual test results are similar to those, which were already described in the previous section in connection with the constant amplitude loading conditions.

For that part of the fatigue live which is spent in stage I (crack-free stage) a non-linear damage accumulation (due to the sequence effects) was also observed. This becomes clearly visible in Fig. 15, where "biharmonic" cycles and besides that a simple block sequence (5 small cycles after 1 larger cycle) were considered. If a simple linear damage calculation analogous to the common Palmgren/Miner-hypothesis[30,31] is performed for stage I using the

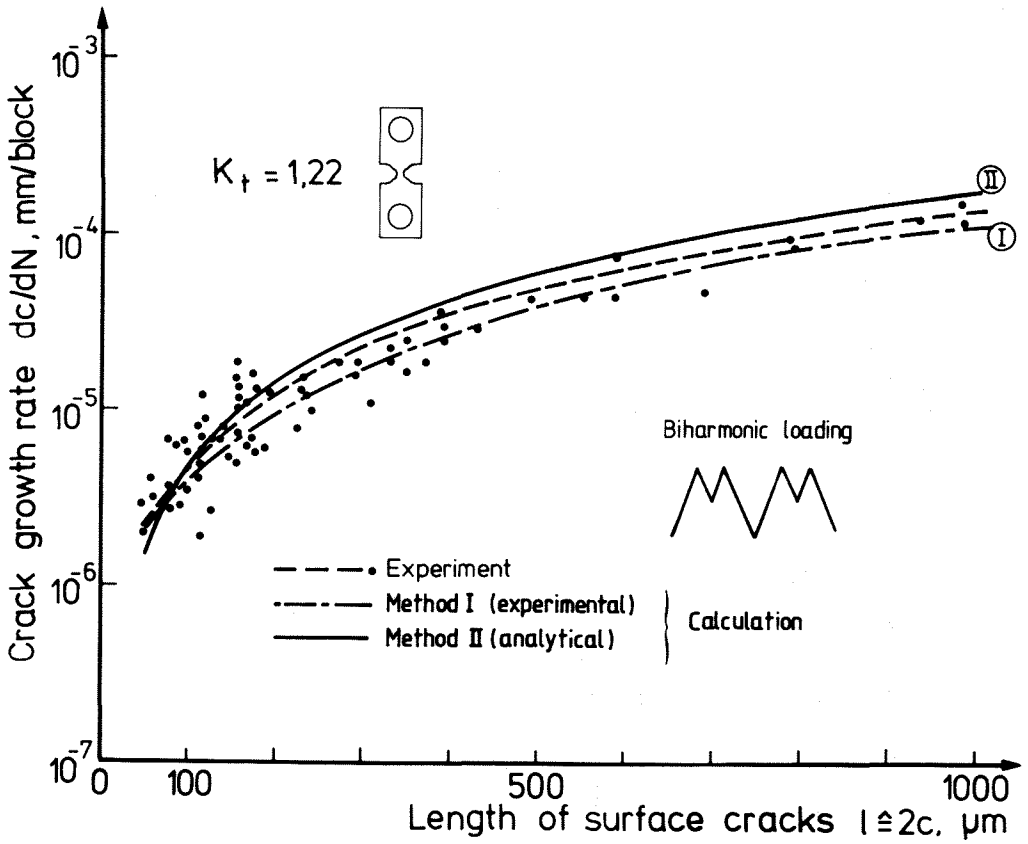

FIGURE 14. Microcrack growth behaviour of the K_t = 1.22 specimens under biharmonic loading.

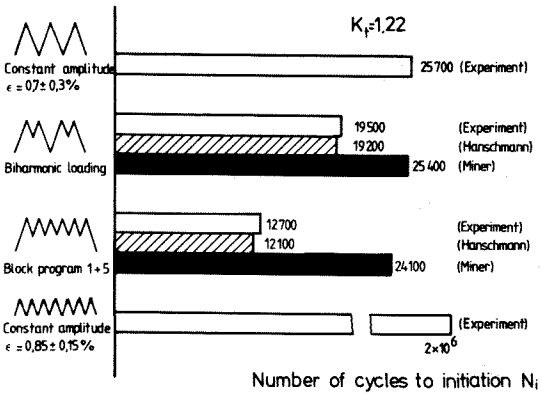

FIGURE 15. Life in the crack initiation stage under constant amplitude loading and under two different types of variable amplitude histories.

following equation:

$$\frac{1}{N_{var.cycl.}} = \frac{1}{N_1} + \frac{n_i}{N_2} \qquad (6)$$

with $n_i = 1$ for the biharmonic cycles and $n_i = 5$ for the (1 + 5)-block sequence and if the constant amplitude data are used which were especially run for stage I and which are also given in the figure. The results after this linear calculation are given in the histogram by the squared regions. It can be seen that these predictions are significantly higher than the actual test results indicating that there are pronounced sequence effects which reduce the life in the actual tests.

In the literature several new approaches have been proposed to consider such sequence effects within the engineering crack initiation stage.[9,10,21] Hanschmann[10] added ZS_i, an additional amount of damage, to the damage per cycle after the common linear damage calculation scheme. ZS_i is:

$$ZS_i = \frac{FWERK \cdot 2 \cdot \ln \frac{N_{\wedge\wedge}}{N_{\wedge\wedge\wedge}}}{\sqrt{k} \cdot \sqrt{N_{\wedge\wedge} \cdot N_{\wedge\wedge\wedge}}} \qquad (7)$$

FWERK is a material constant (for Al 2024-T3 FWERK was found to be about 0.33) and k is a special cycle counter which accounts for the decreasing effect of a high loading with increasing number of smaller cycles after the high loading. $N_{\wedge\wedge}$ and $N_{\wedge\wedge\wedge}$ are the cycle numbers to crack initiation as they were observed in strain controlled constant amplitude tests on unnotched specimens (with the same strain amplitudes and mean strains as for the cycles the predictions have to be made for). If the life values in stage I are calculated by the following equation:

$$\frac{1}{N_{var.cycl.}} = \frac{1}{N_{\wedge\wedge}} + \frac{1}{N_{\wedge\wedge\wedge}} + C \cdot \sum_{i=1}^{n_i} \frac{1}{\sqrt{i}} \qquad (8)$$

$$\frac{1}{N_{Miner}} \quad \text{(compare equ. (6))}$$

the results which are also given in Fig. 15 as hatched regions are achieved. It can be seen that the predictions coincide quite well with the actual test results.

Conclusions

In the present study the fatigue behaviour in the pre-crack and in the microcrack stage was investigated for constant amplitude loading conditions as well as for simple block programmehistories. The experiments were performed on Al 2024-T3 sheets. Three different types of specimens were used, one unnotched (K_t = 1.0) specimen and two types of notched specimens (K_t = 1.22 and K_t = 3.3).

In the tests the same strain histories were applied at the gage length of the unnotched specimens and at the notch root of the notched specimens. In these investigations the following results were found:

Crack initiation

- The microcracks usually started at the hard Fe- and Si-containing intermetallic inclusions.

- Comparisons of the fatigue behaviour of notched and of unnotched specimens (with always the same strain histories at the fatigue critical locations) indicated that the equivalence in the fatigue behaviour became less as the cracks grew larger and, also, when the strain level in the tests was lower.

Propagation behaviour of small cracks

- Fracture mechanics based analyses led to satisfactory predictions of the growth behaviour of small cracks, if the influences of:

  - the crack geometry

  - the stress gradient, and

  - plasticity effects

  were adequately taken into account.

Variable amplitude loading conditions

- Under variable amplitude loading conditions load sequence effects on the crack propagation occured as they are known from long crack experiments. The growth behaviour of the small cracks could be predicted well, if the plasticity effects and the crack opening behaviour were considered.

- In the pre-crack stage sequence effects were also observed. These could be considered if the damage parameter concept after Hanschmann was applied.

Acknowledgements

The financial support of the DFG (Deutsche Forschungsgemeinschaft) and the help of H.J. Strunck and K.H. Trautmann regarding the performance of the experimental studies are greatfully acknowledged.

References

(1) Kellerer, H. and Winkler, P.J.: "Werkstoffe in der Luft- und Raumfahrt, Stand und Tendenzen", Metall, 32 (1978) 7, pp. 696-702.

(2) Schütz, W.: "Fatigue Crack Growth", AGARD Lecture Series No. 97, "Fracture Mechanics Design Methodology" (1979), pp. 3.1-3.13.

(3) Foth, J., Nowack, H. and Lütjering, G.: Proc. 4th Eur. Conf. on Fract., Leoben/Austria (1982).

(4) Miller, K.J.: "The Short Crack Problem", Fat. Eng. Mats. Structs., Vol. 5 (1982) No.3, pp. 223-232.

(5) Lankford, J.,: "The Growth of Small Fatigue Cracks in 7075-T6 Aluminum", Fat. Eng. Mats. Structs., Vol. 5 (1982) No. 3, pp. 233-248.

(6) N.N.: "Behaviour of Short Cracks in Airframe Components", AGARD Conference Proceedings No. 328 (1983).

(7) Taylor, D. and Knott, J.F.,: "Fatigue Crack Propagation Behaviour of Short Cracks; The Effect of Microstructure", Fat. Eng. Mats. Structs., Vol. 4 (1981) No. 2, pp. 147-155.

(8) Kitagawa, H., Tkahashi, S., Suh, C.M. and Miyashita, S.: "Quantitative Analysis of Fatigue Process- Microcracks and Slip Lines under Cyclic Strains", ASTM-STP 675, Am. Soc. Test. Mats.(1979), pp. 420-449.

(9) Nowack, H., Hanschmann, D., Foth, J., Lütjering, G. and Jacoby, G.: "Prediction Capability and Improvements of the Numerical Notch Analysis for Fatifue Loaded Aircraft and Automotive Components", ASTM-STP 770, Am. Soc. Test. Mats. (1982), pp. 269-295.

(10) Hanschmann, D.: "Ein Beitrag zur rechnerischen Anrißlebensdauervorhersage schwingbeanspruchter Kraftfahrzeugbauteile aus Aluminiumwerkstoffen", Dissertation, TH Aachen (1981), also DFVLR-FB 81-10 (1981).

(11) Schijve, J.: "Lecture Notes on Fatigue, Static Tensile Strength and Stress Corrosion of Aircraft Materials and Structures", TH Delft Report LR-360 (1982).

(12) Schulte, K. and Nowack, H.: "Influence of Monotonic and Cyclic Predeformation on Fatigue Crack Propagation of High-Strength Aluminum Alloys", Eng. Fract. Mech., Vol. 13 (1980), pp. 1009-1021.

(13) Crews, J.H. and Hardrath, H.F.: "A Study of Cyclic Plastic Stresses at a Notch Root", Exp. Mech. 23 (1966), pp. 313-320.

(14) Foth, J.: "Einfluß von einstufigen und nichteinstufigen Schwingbelastungen auf Rißbildung und Mikrorißausbreitung in Al 2024-T3", Dissertation, TU Hamburg-Harburg (1983).

(15) Grosskreutz, J.C.: "Fatigue Mechanisms in the Sub-Creep Range", ASTM-STP 495, Am. Soc. Test. Mats. (1971), pp. 5-60.

(16) Lütjering, G., Döker, H. and Munz, D.: "Microstructure and the Fatigue Behaviour of Al-Alloys", "The Microstructure and Design of Alloys 1", (1973), pp. 427-431.

(17) Bowles, C.Q. and Schijve, J.: "The Role of Inclusions in Fatigue Crack Initiation in an Aluminum Alloy", Int. Journ. Fract., Vol. 9, No. 2 (1973), pp. 171-179.

(18) Lankford, J. and Kusenberger, F.N.: "Initiation of Fatigue Cracks in 4340 Steel", Met. Trans. 4 (1973), pp. 553-559.

(19) Foth, J., Marissen, R., Nowack, H. and Lütjering, G.: "A Fracture Mechanics Based Description of the Propagation Behaviour of Small Cracks at Notches", Proc. 5th Eur. Conf. on Fract., to be held at Lisboa/Portugal (1984).

(20) Ott, W.: "Elastisch-plastische FE-Analyse an Kerben", Report "Betriebsfestigkeit von Leichtbauwerkstoffen", DFVLR, Köln (1982).

(21) Nowack, H., Hanschmann, D. and Trautmann, K.H.: "Numerical Crack Initiation Life Prediction for Low Weight Constructions: A Critical State of the Art Survey", Report Int. Symp. "Kurzzeit-Schwingfestigkeit und elastoplastisches Werkstoffverhalten", Stuttgart (1979), pp. 331-354.

(22) Crews, J.H., Jr.: "Crack Initiation at Stress Concentrations as Influenced by Prior Local Plasticity", ASTM Symp. "Achievement of High Fatigue Resistance in Metals and Alloys", Atlantic City, New Jersey (1969).

(23) Elber, W.: "The Significance of Fatigue Crack Closure", ASTM-STP 486, Am. Soc. Test. Mats. (1971), pp. 230-242.

(24) Newman, J.C.,Jr. and Raju, I.S.: "An Empirical Stress Intensity Factor Equation for the Surface Crack", Eng. Fract. Mech., Vol. 15 (1981), pp. 185-192.

(25) Tada, H., Paris, P.C. and Irwin, G.R.: "The Stress Analysis of Cracks Handbook", Del Research Corp., St. Louis/USA (1973).

(26) Rice, J.R.: "Fracture- An Advanced Treatise, Mathematical Fundamentals", Vol. 2, Acad. Press, New York (1968), p. 191.

(27) Shih, C.F. and Hutchinson, J.W.: "Fully Plastic Solutions and Large Scale Yielding Estimates for Plane Stress Crack Problems", Journ. Eng. Mats. Techn. (1976), pp.289-295.

(28) Schijve, J.: "Prediction of Fatigue Crack Growth in 2024-T3 Alclad Sheet Specimens under Flight-Simulation Loading", TH Delft, The Netherlands, Memorandum M-415 (1981).

(29) Marissen, R., Trautmann, K.H. and Nowack, H.: "Analysis of Sequence Effects under Variable Amplitude Loading on the Basis of Recent Crack Propagation Models", TMS-AIME Fall Meeting, St. Louis/USA (1982).

(30) Palmgren, A.: "Die Lebensdauer von Kugellagern", VDI-Z 69 (1929), pp. 337-341.

(31) Miner, M.: "Cumulative Damage in Fatigue", Journ. of Appl. Mech. (1945), A., pp. 159-169.